ACS OMEGA

http://pubs.acs.org/journal/acsodf

Article

Lectin-Fortified Cationic Copper Sulfide Nanoparticles Gain Dual Targeting Capabilities to Treat Carbapenem-Resistant *Acinetobacter baumannii* Infection

Dharshini Karnan Singaravelu, Dalal Nasser Binjawhar, Fuad Ameen, and Anbazhagan Veerappan*

Cite This: *ACS Omega* 2022, 7, 43934−43944

Read Online

ACCESS | Metrics & More | Article Recommendations | Supporting Information

ABSTRACT: Targeted drug delivery maximizes the chance to combat infection caused by drug-resistant pathogens. Herein, lectin-fortified cationic copper sulfide (cCuS) nanoparticles were suggested for targeted adhesion to bacterial membranes and to enforce bacterial death. Jacalin, a lectin from jackfruit seed, was conjugated to fluorescein isothiocyanate (FITC), and its ability to recognize bacterial cell surface glycans was demonstrated. Jacalin formed a noncovalent complex with cCuS, which was investigated by fluorescence quenching measurements. The data revealed that jacalin−cCuS (JcCuS) had a good affinity with an association constant K_a of 2.27 (± 0.28) × 10^4 M^{-1}. The resultant JcCuS complex displayed excellent anti-infective activity against carbapenem-resistant *Acinetobacter baumannii* (CRAB). The minimum inhibitory concentration (MIC) of cCuS was 62.5 μM, which was 2-fold lower than that of the broad-spectrum antibiotic ciprofloxacin. Interestingly, the MIC of JcCuS was reduced to 15.63 μM, which was attributed to jacalin fortification. The mechanistic study unveiled that JcCuS affected the membrane integrity, depolarized the inner membrane, and produced excess reactive oxygen species to combat CRAB at a lower concentration compared to cCuS. *A. baumannii* formed a biofilm more readily, which played a critical role in pathogenesis and resistance in clinical settings. JcCuS (3.91 μM) displayed stronger antibiofilm activity without affecting the metabolic viability of CRAB. Microscopy analyses confirmed the inhibition of biofilm formation and disruption of the mature biofilm upon treatment with JcCuS. Furthermore, JcCuS hindered pellicle formation and inhibited the biofilm-associated virulence factor of CRAB such as exopolysaccharide, cell surface hydrophobicity, swarming, and twitching mobility. The anti-infective potential of JcCuS was demonstrated by rescuing CRAB-infected zebrafish. The reduction in pathogen proliferation in muscle tissues was observed in the treated group, and the fish recovered from the infection and was restored to normal life within 12 h. The findings illustrate that lectin fortification offers a unique advantage in enhancing the therapeutic potential of antimicrobials against human pathogens of critical priority worldwide.

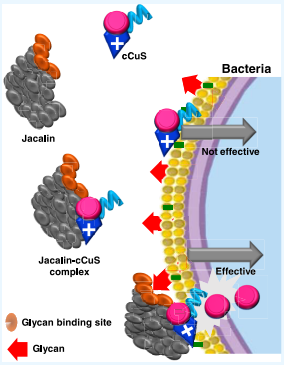

INTRODUCTION

Acinetobacter baumannii is a predominant Gram-negative bacterium responsible for hospital-acquired nosocomial infection.[1] *A. baumannii* is opportunistic bacteria that may be found on the skin or in water, food, and soil. It can survive on dry filter paper for six days, on glass surfaces for more than seven days, and on cotton for more than 25 days.[2] It causes life-threatening conditions like pneumonia, blood infection, meningitis, urinary tract infection, and skin and wound infection.[3] *A. baumannii* infection was treatable with different classes of antibiotics such as β-lactams, aminoglycosides, and tetracyclines.[4] However, some strains can no longer be treated by first-line antibiotics. Hence, last-line antibiotics like carbapenems are used. The World Health Organization (WHO) issued a red alert for *A. baumannii* infection because >50% of clinically isolated Acinetobacter strains are resistant to multiple antibiotics including carbapenems.[5] The increasing identification of carbapenem-resistant *A. baumannii* (CRAB) isolates limits therapeutic options causing substantial morbidity and mortality. CRAB evades antibiotic therapy by adopting a biofilm mode of survival. The rate of biofilm formation of Acinetobacter strains is significantly higher (80−91%) than the other species.[6] Hence, novel therapeutic interventions that can overcome the biofilm virulence factor are required to combat the *A. baumannii* infection.

Recent development in nanotechnology reports nanoparticles (NPs), such as Ag, Au, Cu, Pd, Pt, CuS, CuO, TiO_2, ZnO, Bi_2O_3, and so forth, to combat biofilm-related infection and planktonic bacterial infection.[7−10] However, the broader application of NPs depends on safe and efficient methods of delivery. An ideal method for exerting effective antimicrobial activity is to use cationic molecules to target the outer envelope of bacteria[11] because most bacterial cell surfaces possess a net negative charge at neutral pH due to the presence of ionizable phosphoryl and carboxylate

Received: August 16, 2022
Accepted: November 4, 2022
Published: November 21, 2022

substituent in the peptidoglycan and lipopolysaccharides of cell walls.[12] *A. baumannii* contains surface carbohydrates such as capsular polysaccharides (capsule), lipooligosaccharide (LOS), and the exopolysaccharide poly-β-(1−6)-*N*-acetylglucosamine (PNAG), which plays a significant role in the overall fitness and virulence.[12] Here, we describe cationic copper sulfide nanoparticles (cCuS NPs) to access the negative cell surface charge of the bacterial membrane and enhance the NP-delivering capacity by fortifying with a glycan-binding protein, jacalin. Jacalin is a tetrameric lectin with an affinity to glycans like galactose, mannose, *N*-acetylgalactosamine, *N*-acetylmuramic acid, and *N*-acetylneruamic acid.[13] Besides glycan binding, jacalin also binds to exogenous ligands like porphyrin, ruthenium complexes, and NPs, thereby offering key advantages of acting as a drug carrier to target cell surface glycans.[14−17] Herein, cationic copper sulfide nanoparticles (cCuS)−jacalin complex (JcCuS) was reported and tested against CRAB. The result showed that jacalin forms a noncovalent complex with cCuS and the binding constant is 3×10^4 M^{-1}. Jacalin−cCuS NPs (JcCuS) are highly effective in killing CRAB with a minimum inhibitory concentration of 15.63 μM, which is 4-fold lower than that of cCuS NPs (62.5 μM). The assay focused on studying the changes in the cell envelope reveals that JcCuS affects the membrane integrity and produces excess reactive oxygen species (ROS) to kill the bacteria.

The antimicrobial accessibility to drug-resistant microorganisms was often affected by biofilms.[18] A biofilm is a community of microorganisms encased in extracellular polymeric substances (EPSs) with a capacity to adhere to biotic and abiotic surfaces and colonizes to persist and resist infection. Surface polysaccharides, especially PNAG, constitute a substantial portion of the biofilm and contribute to *A. baumannii* pathogenicity.[19] Hence, drugs fortified with lectin were chosen to access the surface polysaccharides for delivering drugs efficiently to curb the biofilm. The minimum biofilm inhibitory concentration (MBIC) determined with cCuS and JcCuS reveals that the MBIC of cCuS (7.81 μM) was reduced 2-fold when the *A. baumannii* biofilm is treated with JcCuS (3.91 μM). The mechanistic study indicates that JcCuS is highly efficient in inhibiting the virulence factors responsible for biofilm formation, which includes cell surface adhesion, EPS production, and motility. Further, through the zebrafish animal model, in vivo anti-infective potential of JcCuS was demonstrated.

RESULT AND DISCUSSION

Jacalin Recognizes Bacterial Cell Surface Glycan through Sugar-Binding Sites. The surface of all living cells contains glycolipids and glycoproteins and therefore represents natural targets for lectin binding.[20] Herein, the carbohydrate specificity of jacalin was explored for drug delivery. Jacalin's ability to bind bacterial membranes was studied using the jacalin−FITC conjugate (JFC). The UV−vis spectral features of jacalin and FITC with absorbance maximum were observed at 280 and 495 nm, respectively (see Figure S1A). In JFC, both the spectral features of the lectin and FITC appeared, indicating the conjugated form. JFC emits the characteristics of FITC fluorescence with emission at 520 nm, which falls in the green spectrum (see Figure S1B). Jacalin has good specificity for galactose.[21] The galactose-bound form JFC showed FITC fluorescence at 520 nm, suggesting that sugar binding to jacalin does not affect the FITC fluorescence. CRAB cells stained with JFC showed green cells when imaged in fluorescence microscopy, even after washing (Figure 1). In contrast, JFC complexes with galactose

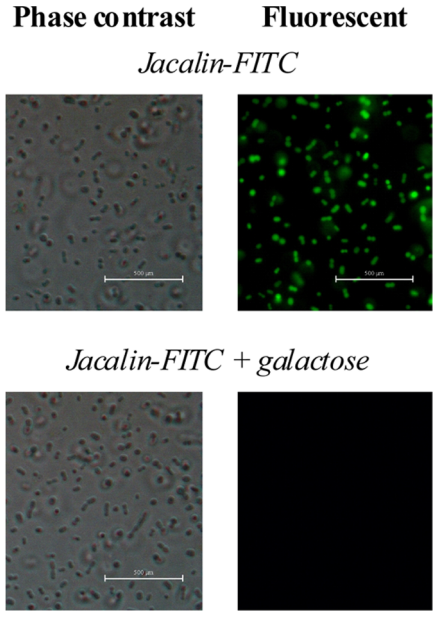

Figure 1. Labeling bacterial membranes using the jacalin−FITC conjugate. Galactose bound to the jacalin−FITC conjugate hinders bacterial labeling. Scale bar: 500 μm.

were unable to stain the cells and showed no fluorescence. These observations suggest that jacalin access the bacterial membranes through its sugar binding, and any hindrance to the sugar-binding site prevents the binding of jacalin to the bacterial membranes.

Preparation of Jacalin−cCuS NPs Complex. Cationic copper sulfide (cCuS) nanoparticles were prepared using the capping agent [2-((*N*-(2-hydroxyethyl)palmitamido)methyl)-1-methylpyridin-1-ium iodide] (cN16E).[22] The surface charge of the NPs was quantitatively described by zeta potential. A positive zeta potential value of +10.0 mV suggested that the effective electric charge of the NP surface was positive, which may aid the NPs in recognizing the negative surface charge of bacteria. To introduce additional targeting capability, cCuS was functionalized with jacalin, while in complex with cCuS, the zeta potential values of jacalin changed from −24.3 to −16.3 mV. The altered zeta potential may be associated with the interaction of lectin on the cCuS surface. The binding affinity between jacalin and cCuS NPs was analyzed by the protein fluorescence quenching method. The fluorophores, tryptophan, and tyrosine present in the jacalin were sensitive to ligand binding.[15−17] It was found that the fluorescence of jacalin was quenched upon titrating with cCuS NPs (Figure 2A). The addition of cCuS NPs quenched the fluorescence maxima at 333 nm with a quenching percentage of 73.0 ± 2.14% at 0.1 mM of cCuS NPs. From the quenching data, the binding curves were plotted using the change in fluorescence.[23] It is noted from Figure 2B that the change in fluorescence (ΔF) increases with increasing concentration of cCuS NPs, displaying saturation behavior at the highest concentration. This suggests that the quenching data are the result of binding between cCuS NPs and jacalin.

The analysis of the fluorescence quenching data by the Stern−Volmer equation yielded a quenching constant (K_{sv}) of

https://doi.org/10.1021/acsomega.2c05252
ACS Omega 2022, 7, 43934−43944

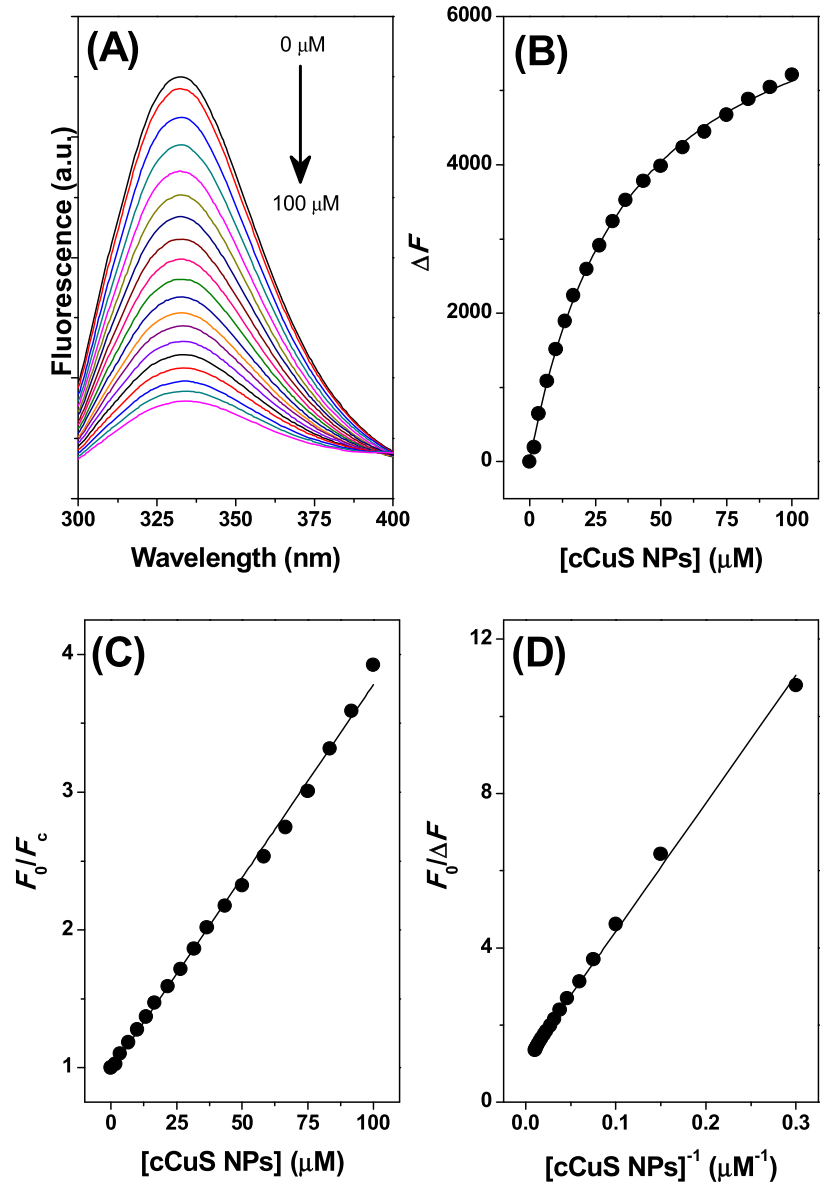

Figure 2. Binding study. (A) Fluorescence quenching titration depicts the interaction of jacalin with cCuS. The first spectrum corresponds to free jacalin and the remaining spectra with decreasing fluorescence emission were obtained in the presence of increasing cCuS concentration. (B) Binding curves show the saturation behavior due to interaction. (C) Stern−Volmer plot, and (D) modified Stern−Volmer plot. Plots correspond to single experiments. The experiments are performed in triplicate, and mean ± standard deviation is reported.

2.62 (± 0.25) × 10^4 M^{-1}. The linearity of the Stern−Volmer plot was attributed to static quenching, where jacalin formed a complex with cCuS NPs in the ground state (Figure 2C).[24,25] The binding constant (K_a) of the JcCuS complex was derived from a modified Stern−Volmer equation as 2.27 (± 0.28) × 10^4 M^{-1} (Figure 2D). The formation of the complex between jacalin and cCuS may block or modify the jacalin−sugar-binding site. To understand the free availability of sugar-binding sites in the JcCuS complex, we carried out binding experiments in the presence of galactose. Jacalin had specificity for galactose, and the sugar-binding site of jacalin was important to recognize the cell surface glycans for drug delivery. The binding studies carried out with jacalin in the galactose-bound form showed a quenching percentage of 80.54 ± 1.22% (see Figure S2). The K_{sv} and K_a were calculated as 4.09 (± 0.32) × 10^4 and 5.71 (± 0.65) × 10^4 M^{-1}, respectively. The K_a (10^4 M^{-1}) obtained for the jacalin−cCuS was comparable to K_a (10^4 M^{-1}) estimated for the jacalin−sugar interaction. This suggested that cCuS was bound to jacalin with similar affinity compared to sugars. Through binding studies, it was evident that cCuS NPs formed noncovalent complexes even in the presence of galactose. The findings also suggested that the cCuS NPs and galactose may bind to jacalin with comparable affinity, but their site of binding to jacalin differed. The effect of cCuS binding to jacalin structure was further analyzed by FTIR (see Figure S3). The characteristic OH stretching, CH stretching, amide I stretching, C═O stretching, and OH bending of jacalin were observed in JcCuS. The observations suggested that the complex formation did not alter the jacalin structure.

Effect of JcCuS against CRAB. The formation of the JcCuS complex with the capacity to target bacterial surface glycans allowed us to investigate the antimicrobial effectiveness of JcCuS. The minimum inhibitory concentration (MIC) of

https://doi.org/10.1021/acsomega.2c05252
ACS Omega 2022, 7, 43934−43944

cCuS NPs and JcCuS against CRAB was discerned from the turbidimetry method (see Figure S4). It was found that the MIC of cCuS NPs against CRAB decreased from 62.5 to 15.63 μM when complexed with jacalin (Table 1). Similar results

Table 1. MIC of the Tested Compounds against CRAB

drug	MIC (μM)
cCuS NPs	62.5
JcCuS	15.63
JcCuS + galactose	62.5
ciprofloxacin	125

were obtained from JcCuS against other Gram-positive and -negative bacteria (see Table S1), suggesting that NPs had broad-spectrum antimicrobial activity. It is worth mentioning that jacalin alone has no antimicrobial activity.[30]

The MIC of JcCuS was 8-fold lower than that of the standard antibiotic ciprofloxacin (MIC-125 μM), indicating that JcCuS was useful in inhibiting CRAB infection at 15.63 μM. However, when JcCuS was in complex with galactose, the MIC of JcCuS was reversed back to 62.5 μM, suggesting that the glycan recognition site was blocked by galactose in JcCuS. To confirm that galactose blocked the antimicrobial activity of JcCuS, a zone of inhibition (ZOI) experiment was carried out at 15.63 μM JcCuS in the absence and presence of galactose (see Figure S5). It is noted from Figure S5 that 15.63 μM JcCuS showed ZOI with a diameter of 14 mm, whereas JcCuS in the presence of galactose showed no ZOI. These findings support that JcCuS uses the sugar recognition site of jacalin to target the bacterial cell surface glycans. The glycan-binding property of jacalin maximizes the delivery of cCuS NPs to exert excellent antimicrobial activity at a 4-fold lower concentration compared to pure cCuS NPs.

Time−kill kinetics assays were used to study the effectiveness of cCuS and JcCuS against CRAB.[26] The bacterial system is exposed to 15.63 μM of the tested molecules and monitored bacterial growth and death over time. It was noted from Figure 3 that the CRAB incubated with JcCuS showed a rapid reduction in the average of the viable cells counted. On the contrary, there was a net growth of bacteria treated with

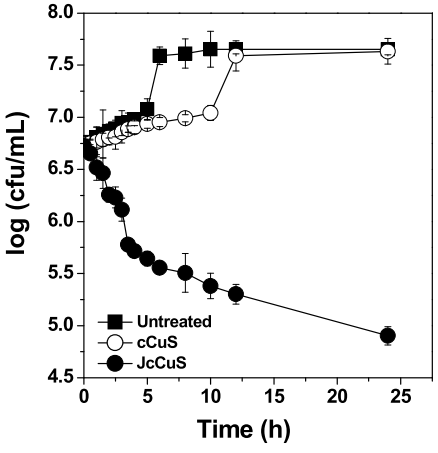

Figure 3. Kill curve. CRAB was challenged with 15.63 μM cCuS and JcCuS. The time course of bacterial killing was followed from 0 to 24 h by determining bacterial colonies, which is represented as $\log_{10}$ cfu/mL. The error bars represent the mean ± standard error from three independent experiments.

cCuS, which was comparable to untreated control. The finding suggests that JcCuS is highly effective in combating CRAB.

Antimicrobial Mechanism. The reason behind the higher effectiveness of JcCuS against CRAB was investigated mechanistically. In the cases of drug-resistant strains, the lipid or protein composition of OM is altered and contributes to the outer membrane (OM) impermeability to drugs.[27] The action of any drug depends on its ability to disturb or cross the bacteria cell envelope. Generally, hydrophobic drugs take a lipid-mediated pathway, and hydrophilic drugs diffuse through porins.[28] The cationic surface charge of cCuS and the glycan-binding properties of jacalin can provide a double advantage to JcCuS to attach to the cell wall of CRAB. The consequence of JcCuS attachment to the cell envelope was analyzed by the acridine orange/propidium iodide (AO/PI) double staining fluorescence imaging method to demonstrate live and dead cells.[29] AO is cell permeates and stains all nucleated cells to produce green fluorescence for live cells, whereas PI is cell impermeant and stains only dead cells with compromised membranes to produce red fluorescence.[30] It is noted from Figure 4 that the cells treated with JcCuS fluoresce red,

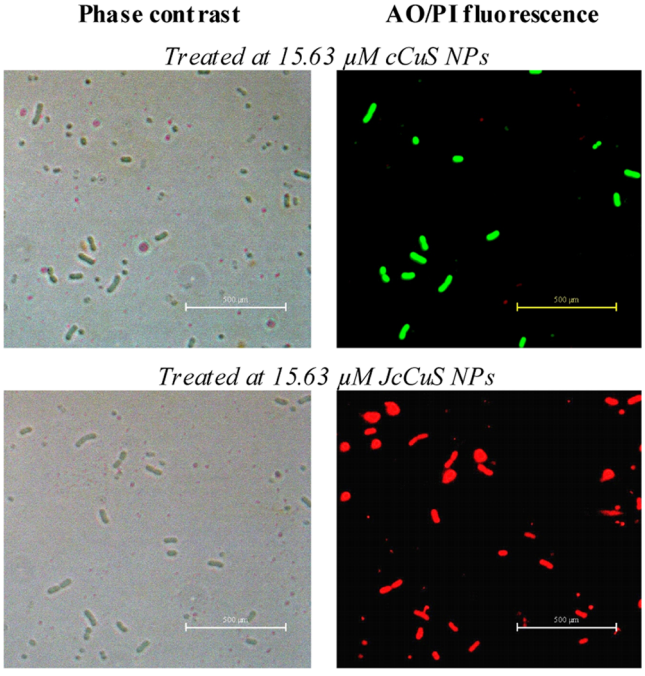

Figure 4. Live and dead staining. CRAB cells were stained with AO/PI fluorophores. Viable cells fluoresce green, and dead cells fluoresce red. Scale bar: 500 μM.

indicating that PI enters the cells due to the loss of membrane integrity and the cells are dead. However, cCuS-treated cells showed green fluorescence due to staining by AO, suggesting that the cells were alive. In addition, the effect of JcCuS on the outer membrane (OM) integrity and inner membrane depolarization was studied by specific fluorophores (see Figure S6). The OM integrity was assayed using the hydrophobic fluorescent dye, *N*-phenyl-1-naphthylamine (NPN).[31] NPN cannot cross the intact outer membrane permeability barrier and emits weak fluorescence in the aqueous environment. The bacterial cells treated with 15.63 μM JcCuS and subsequent exposure to NPN showed strong fluorescence, whereas 15.63 μM cCuS NPs showed weak fluorescence (see Figure S6A).

https://doi.org/10.1021/acsomega.2c05252
ACS Omega 2022, 7, 43934−43944

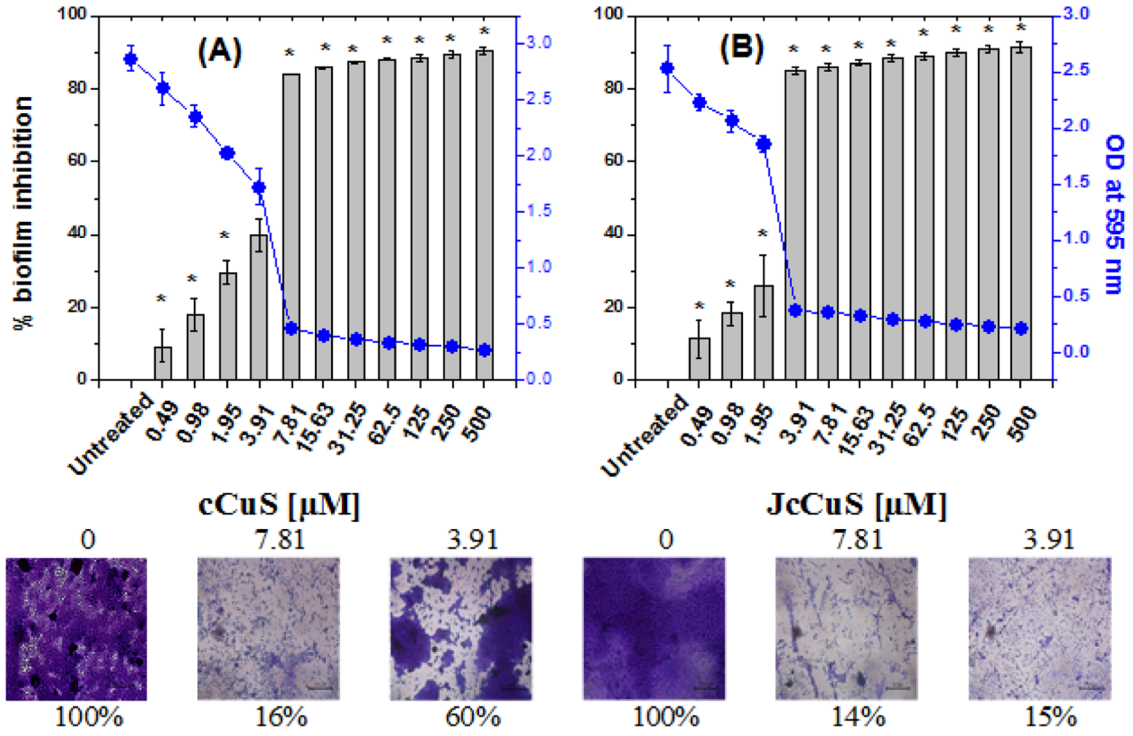

Figure 5. Effect of (A) cCuS and (B) JcCuS at various concentrations on the growth (blue dots) and biofilm formation (gray bar) of CRAB. Error bars indicate SD. * indicates statistical significance ($p < 0.05$) analyzed by the one-way ANOVA method. Bottom panel: light microscopy image represents the biofilm formed on a glass surface and inhibited by cCuS and JcCuS at the tested concentration.

This suggests that JcCuS disturbs the OM permeability barrier of CRAB and allows the NPN to gain access to lipid layers to emit strong fluorescence.

The cell membranes of viable bacteria are polarized due to the negative transmembrane potential.[32] The dissipation of transmembrane potential may kill the bacteria.[33] The ability of JcCuS to depolarize the CRAB membranes was investigated using a membrane potential-sensitive fluorophore, 3,3′-dipropylthiadicarbocyanine iodide [DiSC3(5)].[34] The cationic dye DiSC3(5) is membrane permeable and emits weak fluorescence when bound to viable cells (see Figure S6B). It is noted from Figure S6B that the CRAB treated with JcCuS showed strong fluorescence due to membrane depolarization, which resulted in dye release. Noteworthy, the cells treated with cCuS NPs do not show membrane depolarization, suggesting that 15.63 μM JcCuS is effective in dissipating the cytoplasmic membrane to kill the bacteria.

Reactive oxygen species (ROS) is an important cell signaling molecule for normal biological processes, but the excessive generation of ROS may induce oxidative stress and damage the cells.[35,36] Hence, the ROS production was investigated in CRAB with and without JcCuS treatment using the dichlorofluorescein diacetate (H_2DCFDA) assay.[37] H_2DCFDA is membrane-permeant and nonfluorescent until the acetate group is cleaved by intracellular esterases and oxidation by ROS. The exposure of H_2DCFDA-loaded CRAB to JcCuS stimulated the strong fluorescence, suggesting that excess generation of ROS upon treatment converted H_2DCFDA to the highly fluorescent dichlorofluorescein (DCF, see Figure S6C). The formation of ROS can result from disruption of the electron transport chain. The cells treated with cCuS NPs did not stimulate strong fluorescence compared to JcCuS, indicating that ROS production was scavenged by natural antioxidants. The higher fluorescence as a result of excess ROS production from JcCuS-treated cells was attributed to the bacterial cell surface glycan targeting ability of jacalin. It is worth mentioning that at higher concentrations (62.5 μM), cCuS overcomes the natural antioxidant defense, produces excess ROS, and disturbs the membrane integrity (see Figure S7). The preference of JcCuS for the negative surface charge of the bacterial membranes and the glycan recognition nature of JcCuS produce excellent antimicrobial activity from JcCuS at a lower concentration. These findings explain that the bacteria's death is due to the formation of ROS, OM permeability, and inner membrane depolarization by JcCuS.

EFFECT OF JCCUS ON THE CRAB BIOFILM

Biofilm Inhibition. CRAB has a higher tendency to adopt a biofilm lifestyle to survive and resist antibiotic treatment.[38] Hence, it is important to discover new antibiofilm agents to improve the sensitivity of bacteria to antibiotics. The biofilm inhibitory activity of cCuS NPs and JcCuS against CRAB was performed by the crystal violet (CV) quantification assay.[39] The minimum biofilm inhibitory concentration (MBIC) is the lowest concentration of antimicrobial agents required to inhibit the formation of the biofilm (>50%). It is noted from Figure 5 that cCuS NPs inhibit the CRAB biofilm at 7.81 μM and JcCuS inhibits at 3.91 μM. The MBIC was lower than the MIC, suggesting that cCuS NPs and JcCuS exhibit true biofilm inhibitory activity without affecting the growth. To confirm that the cells are viable at MBIC, a resazurin microtitre assay (REMA) plate was performed (see Figure S8). In REMA, the nonfluorescent dye resazurin undergoes chemical reduction to red-fluorescent resorufin in metabolically active cells.[40] The obtained data showed that the cells treated at MBIC turn the

https://doi.org/10.1021/acsomega.2c05252
ACS Omega 2022, 7, 43934−43944

blue color nonfluorescent resazurin into fluorescent red color resorufin using the natural reducing power of viable cells (see Figure S8). It is worth noting that the cells treated at MIC were unable to respirate and the resazurin remained blue. This suggested that cell growth was not affected at MBIC and the growth was only affected at MIC. JcCuS at a concentration of 3.91 μM showed strong antibiofilm activity with 85% inhibition, whereas at the same concentration, cCuS NPs showed weak antibiofilm activity with 40% inhibition (Figure 5). In addition to the CV quantification assay, the biofilm formed on a glass surface was analyzed by light microscopy. CRAB control samples grown on a glass plate showed highly aggregated and well-structured biofilm formation (Figure 5). The microscopy image showed that samples treated with 3.91 μM JcCuS disturbed the biofilm formation, and dispersed cells were observed, whereas the 3.91 μM cCuS NP-treated sample retained a considerable amount of the biofilm. However, CV-stained imaging illustrated that cCuS NPs at a concentration of 7.81 μM inhibited biofilm formation, which corroborated with the CV quantification assay. The results revealed that JcCuS treatment was more effective in inhibiting CRAB biofilm formation at a lower concentration than cCuS NPs.

Pellicle Inhibition. *A. baumannii* has the ability to colonize at the air−liquid interface to form a biofilm by a process called pellicle formation.[41] Hence, the inhibitory effect of cCuS NPs and JcCuS on the pellicle formation of CRAB was investigated. It is noted from Figure 6 that the untreated CRAB formed

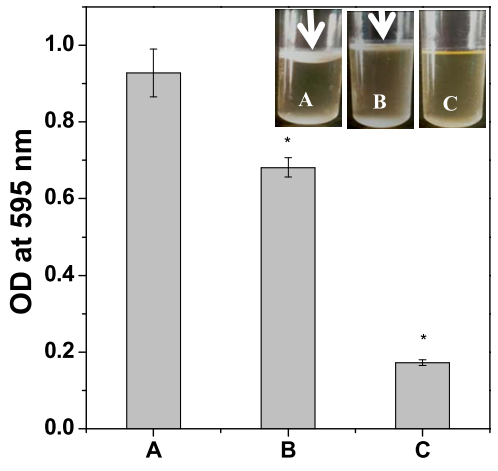

Figure 6. Pellicle inhibition. The CRAB strain was grown in the presence or absence of cCuS and JcCuS for 72 h a 37 °C under static conditions. (A) Untreated, (B) exposed to 3.9 μM cCuS, and (C) exposed to 3.9 μM JcCuS. The bar graph represents pellicle formation as determined by spectrophotometry at OD_{595nm}. The inset provides the digital photograph evidence for pellicle formation and inhibition at the tested conditions. Error bars indicate mean ± SD, and * indicates statistical significance ($p < 0.05$) versus untreated control. The photographs were taken by the author D.K.S.

robust pellicles at the air−liquid interface of the static solution, and this was significantly inhibited by 3.91 μM JcCuS, whereas 3.91 μM cCuS NPs showed moderate ring formation compared to the control; nevertheless, the observation suggests that the cCuS NP activity is weaker compared to JcCuS. The amount of the pellicle material was assessed by collecting the floated material. The optical density of the pellicle material collected from the untreated culture remains higher compared to cCuS and JcCuS treatment (Figure 6). Interestingly, the cell culture exposed to JcCuS showed significantly lower optical density than cCuS, indicating superior pellicle-inhibiting activity to JcCuS. In addition, JcCuS effectively inhibit the adherence of CRAB on glass and the polypropylene surface, as demonstrated by CV staining (see Figure S9). The findings support that the lectin functionalization offers an additional edge to inhibit pellicle formation at a lower concentration.

Biofilm Eradication. Without inhibitors, bacteria adhering to the surface may form a mature biofilm. The mature biofilm resists most antimicrobials and their removal is more challenging. The minimum biofilm eradication concentrations (MBECs) of cCuS NPs and JcCuS NPs were determined by the CV assay (see Figure S10). The MBECs of cCuS NPs and JcCuS NPs were 31.25 and 15.63 μM, respectively.

EFFECT OF JCCUS ON BIOFILM-ADHERENCE FACTORS

Exopolysaccharide Production and Cell Surface Hydrophobicity. The extracellular biofilm matrix is composed of a mixture of polysaccharides, proteins, and nucleic acids.[42] The exopolysaccharide (EPS) component provides a structural scaffold for biofilm formation and also provides a barrier to bacteria against antibiotic penetration and host immune defense. The spectrophotometric analysis of EPS production in the treated samples indicated a considerable reduction in EPS. At the MBIC of JcCuS (3.91 μM), more than 78% reduction in EPS was observed, whereas cCuS NPs (3.91 μM) reduced only 46% when compared to the untreated sample (Figure 7). Cell surface hydrophobicity (CSH) is an

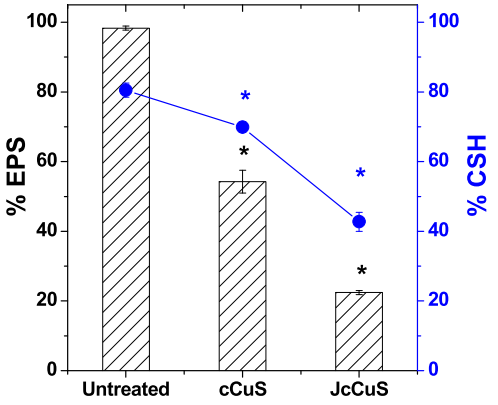

Figure 7. Inhibitory effect of cCuS and JcCuS on (A) EPS production and (B) CSH of CRAB. The error bar represents the mean ± SD. * indicates the statistical significance ($p < 0.05$) with respect to untreated control. All experiments are performed in triplicate.

important virulent factor that contributes to cell adhesion to both biotic and abiotic surfaces.[43] The effect of cCuS NPs and JcCuS on the CSH of CRAB was examined by microbial adhesion to the hydrocarbon (MATH) assay. A significant reduction in the CSH of the samples treated with both cCuS NPs and JcCuS was observed. Interestingly, a higher percentage of reduction in CSH was noted with JcCuS treatment when compared to control and cCuS NP treatment (Figure 6). This result confirmed that jacalin has a significant contribution to the activity of JcCuS to prevent EPS production and reduce the CSH to inhibit the biofilm formation at beginning of the adhesion stage.

https://doi.org/10.1021/acsomega.2c05252
ACS Omega 2022, 7, 43934−43944

Motility Assay. The motility of pathogens is important for initial attachment to host cells and supports internal colonization during pathogenesis. Generally, *A. baumannii* is considered nonmotile due to the lack of flagella, but recent studies showed that *A. baumannii* displays two forms of motility known as swarming and twitching.[44] Therefore, we assessed the influence of JcCuS on the swarming motility and twitching motility. It was found that CRAB displayed a swarming motility of 7 mm in the first 24 h, which increased to 39 mm in 96 h. At 3.91 μM concentration of cCuS NPs, swarming motility was reduced to 5 mm in the first 24 h and 31 mm in 96 h. Strikingly, 3.91 μM JcCuS inhibited the coordinated translocation of the bacterial population across the surface to a greater extent over the tested period (Figure 8).

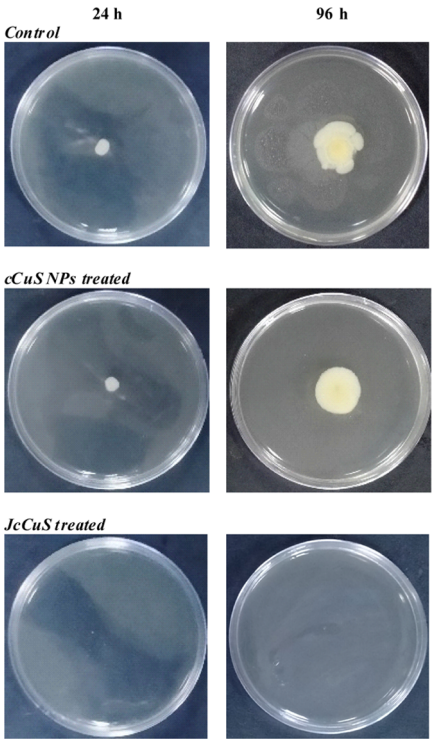

Figure 8. Effect of 3.91 μM cCuS and 3.91 μM JcCuS on the swarming motility of CRAB. The photographs were taken by the author D.K.S.

The surface-associated bacteria movement over moist surfaces, known as twitching motility, was inhibited excellently by 3.91 μM JcCuS compared to cCuS NPs (see Figure S11). The results revealed that the JcCuS action mechanism involves inhibition in EPS production, reduced CSH, and motility inhibition to prevent the adherence potential at the initial stage of biofilm formation.

Anti-infective Activity of JcCuS. The in vitro study clearly showed that JcCuS had excellent antimicrobial and antibiofilm activity. Hence, we analyze the efficacy of JcCuS in treating infective hosts. Zebrafish (*Danio rerio*) genome reveals that 84% of genes associated with human diseases are conserved between humans and zebrafish.[45,46] Thus, zebrafish were considered for this study. It is an easily accessible, well-validated animal model for studying drug effects. Healthy zebrafish were infected intramuscularly with CRAB and divided into two groups: Group A and Group B. Group A was left untreated, and Group B was treated after 3 h of infection with 15.63 μM JcCuS. Group A succumbed to infection in less than 10 h, whereas Group B responded to the JcCuS treatment and survived the infection. To determine the anti-infective effect of JcCuS against CRAB, the bacterial load in the muscles was assessed by the colony count method. To make colony counts in the muscles, the fish from both groups were collected at a defined time point, sacrificed, digested, diluted, and then platted on a sterile agar plate. It is noted from Figure 9 that the number of colony-forming units (CFUs) is

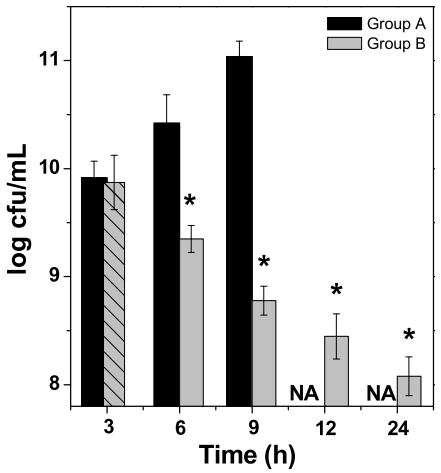

Figure 9. Infected zebrafish treatment. Zebrafish infected with 10 μL of 0.5 OD_{600nm} CRAB. Group A, untreated—succumbed to infection in <10 h. Group B was administered with 10 μL of 15.63 μM JcCuS after 3 h post infection. At a defined point, the bacterial colonies spread in the muscle tissue were determined using the LB agar plate method. NA—fish not alive. The error bar represents the mean ± SD. * indicates a statistically significant difference in measured values when compared to Group A at a defined time point (determined using Student's *t*-test, $p < 0.05$).

the same in both groups at the third hour of infection. In Group A, the CFU increases in the untreated fish over time, suggesting the infection spreading throughout the animal, which resulted in killing the fish in <10 h. Group B treated with 15.63 μM JcCuS showed a 1.1 log-fold reduction in CFU at the first 3 h of treatment and decreased further over time. Noteworthy, the infected fish treated with 15.63 μM cCuS NPs/ciprofloxacin succumbed to infection because the MICs of cCuS NPs and ciprofloxacin were 61.25 and 125 μM, respectively (see Figure S12). This suggests that the 15.63 μM JcCuS treatment effectively reduces the bacterial bioburden from the fish tissues, which allows the fish to rescue completely from CRAB infection.

Biocompatibility Experiments. Hemolysis is a widely used procedure to evaluate hemocompatibility. The hemolysis activities were monitored spectrophotometrically by measuring free hemoglobin and determining the percent heme release after incubating the RBC with the drug. The freshly collected RBC was exposed to NPs with and without jacalin at various MICs. The positive control, Triton X-100, damaged the RBC membranes and released hemoglobin, whereas the tested molecules were unable to leak hemoglobin (Figure S13). The result suggested that the molecules were hemocompatible even at 8× MIC. In vivo compatibility was studied using zebrafish. Fish injected intramuscularly with the NPs remained safe and alive. Further, the biochemical assay of the liver (carboxylesterase, CE) and brain (acetylcholinesterase, ACE) enzyme

https://doi.org/10.1021/acsomega.2c05252
ACS Omega 2022, 7, 43934−43944

revealed that cCuS and JcCuS had no effect on the enzyme activity (see Figure S14). Similar results were reported with platinum NPs.[9] These findings indicate that the NPs are nontoxic and have the potential to explore in vivo biomedical science.

CONCLUSIONS

In summary, the present study, for the first time, revealed the true antibiofilm efficiency of JcCuS against CRAB without affecting growth. Hence, the possibility of drug resistance against JcCuS will be limited. In vitro assays confirmed that JcCuS affected the biofilm-associated adherence factors such as EPS, CSH, swarming, and twitching. Besides antibiofilm activity, JcCuS displays excellent antimicrobial activity by damaging the bacterial membrane and producing excess ROS. Especially, JcCuS exhibits antimicrobial activity at a 4-fold lower concentration compared to cCuS, suggesting that the lectin plays a major role in the enhanced susceptibility of CRAB to JcCuS. Notably, JcCuS treatment was effective in reducing the in vivo colonization of CRAB in zebrafish and rescuing the fish from infection. The hemolytic study and the in vivo toxicity assay suggest that JcCuS is nontoxic. Further study with model membranes may explain the specificity of JcCuS to bacteria over mammalian membranes. Considering the lectin's role in maximizing the antimicrobial and antibiofilm combination effect of cCuS on CARB, it could be a promising strategy to tackle drug-resistant pathogens listed by the world health organization.

EXPERIMENTAL SECTION

Preparation of Jacalin−FITC Conjugates for Imaging. Jacalin from the jackfruit seeds was isolated using a cross-linked guar gum column as described previously. The purity of the lectin was checked by polyacrylamide gel electrophoresis. The concentration of the jacalin was estimated by the Lowry assay using bovine serum albumin as standard. About 1 mg/mL fluorescein isothiocyanate (FITC) dissolved in DMSO was allowed to react with 1 mg/mL jacalin at 4 °C, pH 8 for 12 h in dark. After the reaction, the unreacted FITC was removed by dialysis. The conjugation of jacalin−FITC (JFC) was confirmed by absorbance and fluorescence spectroscopy. For labeling, 50 μL of JFC was incubated with 0.5 OD CRAB for 30 min in dark, and the labeled cells were collected by centrifugation at 3000 rpm for 10 min. The cells were washed twice with PBS and resuspended in PBS for visualization in a Nikon Eclipse fluorescence microscope using a green filter.

Binding of cCuS to Jacalin. The 2-((*N*-(2-hydroxyethyl)-palmitamido)methyl)-1-methylpyridin-1-ium iodide-capped copper sulfide (cCuS) nanoparticles were prepared as described previously.[22] The binding between jacalin and cCuS was monitored in a JASCO-FP8200 spectrometer. Briefly, 5 μM jacalin (3 mL) was titrated by adding small aliquots of 1 mM cCuS, and the change in jacalin fluorescence was monitored from 300 to 400 nm in a quartz cell upon excitation at 280 nm. The fluorescence data were analyzed using Stern−Volmer (eq 1) and modified Stern−Volmer (eq 2) equations.

$$F_0/F_c = 1 + K_{sv}[\text{cCuS}] \quad (1)$$

$$F_0/\Delta F = f_a^{-1} + (K_a f_a)^{-1}\cdot[\text{cCuS}]^{-1} \quad (2)$$

where F_0 and F_c are the fluorescence intensities in the absence and presence of cCuS, respectively, K_{sv} is the Stern−Volmer quenching constant, ΔF is the difference in fluorescence intensity in the presence of cCuS, f_a refers to the fraction of the total fluorophores accessible to the drug, and K_a is the association constant. The slope gives $(K_a f_a)^{-1}$, and their ordinate intercepts give the values of f_a^{-1}.

Antimicrobial Activity. The antimicrobial activity of cCuS and JcCuS was tested against carbapenem-resistant *A. baumannii* (MTCC-12889) obtained from Microbial Type Culture Collection and Gene Bank (MTCC), India, following Clinical & Laboratory Standards Institute (CLSI) guidelines. The JcCuS complex was prepared by incubating the desired concentration of cCuS with 50 μM jacalin for 1 h at 4 °C. The broth microdilution method was performed to determine the MIC. Briefly, 100 μL of the antimicrobial was added to the first well of the 96-well plate and serially diluted using 100 μL of PBS. About 50 μL of 5×10^6 cfu/mL bacterial cells and 50 μL of Luria-Bertani (LB) broth were added to each well and incubated in a shaking incubator at 37 °C. After 24 h of incubation, the optical density of the culture present in each well was read at 600 nm in a microtiter plate reader (Thermo Scientific Multiskan EX). In addition to turbidometric measurement, the MIC was determined by the resazurin microtitre plate assay, where the treated cells were mixed with 30 μL of resazurin (0.01% wt/vol) and incubated at 37 °C for 2 h. The minimum concentration of drugs that induce the color change from blue to pink was noted as MIC. Further, a zone of inhibition assay was performed to demonstrate the antimicrobial efficiency of JcCuS. Typically, 5×10^6 cfu/mL bacterial cells were swabbed on a sterile LB agar plate using sterile cotton swabs. Size wells (10 mm) were constructed using gel puncture and loaded with 50 μL of cCuS or JcCuS. After overnight incubation at 37 °C, the zone formed around the well was measured and reported.

The killing efficiency of JcCuS was determined by time−kill curve analysis. Briefly, CRAB (5×10^6 cfu/mL) grown in LB medium was exposed to 15.63 μM cCuS/JcCuS at 37 °C. Untreated cells were considered as a control. At a defined time interval, the untreated and treated cultures were collected and plated on an LB agar plate with suitable dilution. The plates were incubated at 37 °C for 12 h, and colonies formed on the plate were counted and reported in cfu/mL.

ANTIMICROBIAL MECHANISM

Membrane Permeabilization Assay. The effect of cCuS and JcCuS on the membrane permeability of CRAB was analyzed by the acridine orange/propidium iodide dual staining method. Briefly, 10^9 cfu/mL CRAB cells were treated with 15.63 μM cCuS/JcCuS for 2 h at 37 °C. Then, the cells were collected by centrifugation at 3000 rpm for 10 min and resuspended in 1 mL PBS buffer. About 10 μL of resuspended cells were stained with 10 μL of 0.5 M AO/PI. After 5 min incubation in dark, the cells were drop-cast on a sterile glass plate and visualized under 100× magnification in a Nikon Eclipse fluorescence microscope. A green filter for AO and a red filter for PI were used.

The effect of cCuS/JcCuS on the outer membrane permeability barrier of CRAB was further analyzed by the 1-*N*-phenylnapthylamine (NPN) uptake assay. Briefly, 10^9 cfu/mL CRAB cells were treated with 15.63 μM cCuS/JcCuS for 2 h at 37 °C. Then, the cells were collected by centrifugation at 3000 rpm for 10 min. The pellet was resuspended in 1 mL of

https://doi.org/10.1021/acsomega.2c05252
ACS Omega 2022, 7, 43934−43944

PBS buffer and mixed with 0.5 M NPN. The cell uptake NPN showed strong fluorescence, which was measured by monitoring emission at 420 nm and excitation at 350 nm. Untreated cells and cells treated with 5 mM Triton X-100 served as negative and positive controls, respectively.

Membrane Depolarization Assay. The effect of cCuS/JcCuS on the depolarization cytoplasmic membrane of CRAB was assessed by a membrane potential-sensitive fluorescent dye, $diSC_3(5)$. CRAB cells cultured overnight grown in LB broth were harvested by centrifugation at 3000 rpm, washed thrice, and diluted to 0.5 OD_{600nm} with HEPES buffer (pH 7.2) containing 250 mM sucrose and 5 mM $MgSO_4$. About 2 mL of the bacterial suspension was mixed with 3 μM $diSC_3(5)$ and incubated for 1 h at 37 °C to maximize the dye uptake. The unbound dyes were removed by washing with HEPES buffer. Then, 15.63 μM cCuS/JcCuS was added to the bacterial suspension containing $diSC_3(5)$. The fluorescence emission was monitored at 670 nm (excitation wavelength = 622 nm). Untreated cells and cells treated with 200 μM Triton X-100 were used as negative and positive controls, respectively.

Reactive Oxygen Species. The generation of ROS in CRAB was analyzed by the dichlorofluorescein diacetate (H_2DCFDA) assay. Briefly, 10^9 cfu/mL CRAB cells were treated with 15.63 μM cCuS/JcCuS for 2 h at 37 °C. Then, the cells were collected by centrifugation at 3000 rpm for 10 min, resuspended in 1 mL of PBS buffer, and then incubated with (30μg/mL) H_2DCFDA at 37 °C for 30 min in dark. The formation of dichlorofluorescein was monitored at an emission wavelength of 670 nm and an excitation wavelength of 622 nm. Untreated cells and cells treated with 500 μM H_2O_2 were used as negative and positive controls, respectively.

Antibiofilm Activity. The minimum biofilm inhibitory concentrations of cCuS and JcCuS against CRAB biofilm were determined by the crystal violet assay. Typically, a 1% overnight culture of CRAB was used to inoculate 200 μM tryptic soy broth (TSB) in a 96-well plate without and with various concentrations of cCuS/JcCuS and incubated at 37 °C for 24 h. After that, the microtiter plates were washed three times with PBS to remove unbound cells, followed by air-drying. Then, the plates were stained with a 0.1% crystal violet solution for 20 min, washed with PBS to remove excess stain, and dried at 60 °C for 20 min. The CV-stained biofilm was extracted using a 30% glacial acetic solution and its absorbance was noted at 595 nm. The percent biofilm inhibition was calculated using the following formula:

$$(\%) = [(A_C - A_T)/A_C] \times 100 \quad (3)$$

where A_C and A_T are the control OD_{595nm} and treated OD_{595nm}, respectively.

For the determination of the minimum biofilm eradication concentration, a 1% overnight culture of CRAB was used to inoculate 200 μM of tryptic soy broth (TSB) in a 96-well plate and incubated at 37 °C for 24 h. After that, PBS buffer containing varying concentrations of serially diluted cCuS and JcCuS was added to the plate and incubated at 37 °C. After 24 h, the planktonic cells were washed with PBS and the biofilm was stained with 0.1% CV. Then, the plates were processed as described above.

For the microscopic analysis, the biofilm assay was carried out in a 24-well plate containing glass slides in the absence and presence of JcCuS for 24 h at 37 °C. The slides were stained with 0.1% CV and imaged at the magnification of 100× under a Nikon Eclipse microscope. For biofilm eradication, the preformed biofilm on a glass slide was treated with JcCuS for 24 h and the CV-stained biofilm was imaged.

Pellicle Assay. The effect of cCuS/JcCuS on biofilm formation of CRAB at the air−liquid interface was assessed at static conditions. Briefly, a 1% overnight culture was added to 3 mL of TSB medium without and with 3.91 μM cCuS/JcCuS in glass test tubes and incubated for 72 h at 37 °C without disturbance. For the quantification of pellicle content, 1 mL of ethanol was added carefully underneath the pellicle material without disturbing the top pellicle layer. The floatable pellicle material was collected and the OD was measured at 595 nm.

ANTIVIRULENCE EFFICACY OF JCCUS

EPS Production. For EPS quantification, overnight culture of CRAB diluted to 1:100 in TSB medium was used. About 100 μL of diluted CRAB cultures were grown in the absence and presence of 3.91 μM cCuS/JcCuS for 24 h at 37 °C. After 24 h, the planktonic cells were removed and the plates were washed three times with PBS. The biofilm adhered to the plate contained EPS, which was extracted with a phenol/sulfuric acid/water (125/650/225 μL) solution. Using eq 3, the percentage of EPS inhibition was calculated by measuring the extract absorbance at 490 nm.

Cell Surface Hydrophobicity. The influence of cCuS/JcCuS on the CSH of CRAS was analyzed by the MATH assay. Briefly, 10^9 cfu/mL CRAB cells were grown in the absence and presence of 3.91 μM cCuS/JcCuS for 2 h at 37 °C. After 2 h, the cells were collected by centrifugation at 3000 rpm and washing with PBS. The washed cells were resuspended in 1 mL of PBS to which 1 mL of toluene was added, vortexed for 10 min, and kept at 4 °C for 24 h for phase separation. After the phase separation, the OD of the aqueous phase was monitored at 600 nm. From the OD values, the CSH was calculated by the following formula:

$$\text{CSH}\ (\%) = 100 \times [1 - (\text{OD after vortex}/\text{OD before vortex})]$$

Motility Assay. The swarming and twitching motility of CRAB was evaluated in a tryptic soy agar (TSA) plate. For the swarming motility assay, a 0.4% TSA plate was prepared without and with 3.91 μM cCuS/JcCuS. About 5 μL of the CRAB overnight culture was placed in the center of the plate and incubated in a static incubator at 37 °C. After incubation, the motility zone was observed and measured at 24 and 96 h. For the twitching motility assay, a 0.8% TSA plate was prepared without and with 3.91 μM cCuS/JcCuS. A sterile toothpick dipped in the CRAB overnight culture was stabbed in the middle region of the plate till the bottom. The plates were incubated in a static incubator at 37 °C for 72 h, and then, the agar was discarded carefully. The plates were washed with PBS and stained with 0.1% CV.

Anti-infective Assay. Zebrafish weighing ∼300 mg, irrespective of sex, was purchased from the local aquarium, Thanjavur, India. Fish were fed a commercial fish diet and allowed to acclimatize to the lab environment for three days in aerated glass tanks containing tap water. For the anti-infective assay, 20 healthy fish were injected intramuscularly with 10 μL of 0.5 OD (10^9 cfu/mL) as described in ref 46. After 3 h, the fish were divided into two groups, Group A served as a control and was treated with PBS. Group B was treated with 10 μL of JcCuS (3.91 μM). At a defined time point, the fish were collected and sacrificed, and the muscle tissues were dissected.

https://doi.org/10.1021/acsomega.2c05252
ACS Omega 2022, 7, 43934−43944

About 30 mg of dissected muscle tissue was homogenized, diluted appropriately, and then plated on a sterile LB agar plate. The plates were incubated for 12 h at 37 °C. The colonies formed on the plates were counted and reported in cfu/mL.

■ ASSOCIATED CONTENT

Supporting Information

The Supporting Information is available free of charge at https://pubs.acs.org/doi/10.1021/acsomega.2c05252.

UV−visible spectra; zeta potential; FTIR; turbidimetry assay; NPN assay; ROS assay; REMA plate; and twitching assay (PDF)

■ AUTHOR INFORMATION

Corresponding Author

Anbazhagan Veerappan − *Department of Chemistry, School of Chemical & Biotechnology, Shanmugha Arts, Science, Technology & Research Academy (SASTRA) Deemed University, Thanjavur 613401 Tamil Nadu, India;* orcid.org/0000-0002-0931-8192; Phone: +91 4362-264101-3689; Email: anbazhagan@scbt.sastra.edu; Fax: +9104362-264120

Authors

Dharshini Karnan Singaravelu − *Department of Chemistry, School of Chemical & Biotechnology, Shanmugha Arts, Science, Technology & Research Academy (SASTRA) Deemed University, Thanjavur 613401 Tamil Nadu, India*

Dalal Nasser Binjawhar − *Department of Chemistry, College of Science, Princess Nourah bint Abdulrahman University, Riyadh 11671, Saudi Arabia*

Fuad Ameen − *Department of Botany and Microbiology, College of Science, King Saud University, Riyadh 11451, Saudi Arabia*

Complete contact information is available at: https://pubs.acs.org/10.1021/acsomega.2c05252

Author Contributions

D.K.S. did the studies, D.N.B. and F.A. designed toxicology studies, and V.A. designed the project. The manuscript was written with the contributions of all authors.

Notes

The authors declare no competing financial interest.

■ ACKNOWLEDGMENTS

V.A. acknowledges the financial support given through the Science and Engineering Research Board, Government of India (CRG/2019/003462). D.K.S. earnestly acknowledges the teaching assistantship from SASTRA Deemed University. The authors thank the central research facility (R&M/0021/SCBT 007/2012-13), SASTRA Deemed University, for the provided infrastructure. The research was also supported by Researchers Supporting Project number (PNURSP2022R155), Princess Nourah bint Abdulrahman University, Saudi Arabia.

■ REFERENCES

(1) Ibrahim, S.; Al-Saryi, N.; Al-Kadmy, I.; Aziz, S. N. Multidrug-resistant *Acinetobacter baumannii* as an emerging concern in hospitals. *Mol. Biol. Rep.* **2021**, *48*, 6987−6998.

(2) Bravo, Z.; Orruño, M.; Navascues, T.; Ogayar, E.; Ramos-Vivas, J.; Kaberdin, V. R.; Arana, I. Analysis of *Acinetobacter baumannii* survival in liquid media and on solid matrices as well as effect of disinfectants. *J. Hosp. Infect.* **2019**, *103*, e42−e52.

(3) Howard, A.; O'Donoghue, M.; Feeney, A.; Sleator, R. D. *Acinetobacter baumannii*: an emerging opportunistic pathogen. *Virulence* **2012**, *3*, 243−250.

(4) Kyriakidis, I.; Vasileiou, E.; Pana, Z. D.; Tragiannidis, A. *Acinetobacter baumannii* Antibiotic Resistance Mechanisms. *Pathogens* **2021**, *10*, 373.

(5) Chen, L. K.; Kuo, S. C.; Chang, K. C.; Cheng, C. C.; Yu, P. Y.; Chang, C. H.; Chen, T. Y.; Tseng, C. C. Clinical Antibiotic-resistant *Acinetobacter baumannii* Strains with Higher Susceptibility to Environmental Phages than Antibiotic-sensitive Strains. *Sci. Rep.* **2017**, *7*, No. 6319.

(6) Gedefie, A.; Demsis, W.; Ashagrie, M.; Kassa, Y.; Tesfaye, M.; Tilahun, M.; Bisetegn, H.; Sahle, Z. *Acinetobacter baumannii* Biofilm Formation and Its Role in Disease Pathogenesis: A Review. *Infect. Drug Resist.* **2021**, *14*, 3711−3719.

(7) Shkodenko, L.; Kassirov, I.; Koshel, E. Metal Oxide Nanoparticles Against Bacterial Biofilms: Perspectives and Limitations. *Microorganisms* **2020**, *8*, 1545.

(8) Wang, L. S.; Gupta, A.; Rotello, V. M. Nanomaterials for the Treatment of Bacterial Biofilms. *ACS Infect. Dis.* **2016**, *2*, 3−4.

(9) Ayaz Ahmed, K. B.; Raman, T.; Anbazhagan, V. Platinum nanoparticles inhibit bacteria proliferation and rescue zebrafish from bacterial infection. *RSC Adv.* **2016**, *6*, 44415.

(10) Sengan, M.; Subramaniyan, S. B.; Arul Prakash, S.; Kamlekar, R.; Veerappan, A. Effective elimination of biofilm formed with waterborne pathogens using copper nanoparticles. *Microb. Pathog.* **2019**, *127*, 341−346.

(11) Epand, R. M.; Walker, C.; Epand, R. F.; Magarvey, N. A. Molecular mechanisms of membrane targeting antibiotics. *Biochim. Biophys. Acta, Biomembr.* **2016**, *1858*, 980−987.

(12) Harding, C. M.; Hennon, S. W.; Feldman, M. F. Uncovering the mechanisms of *Acinetobacter baumannii* virulence. *Nat. Rev. Microbiol.* **2018**, *16*, 91−102.

(13) Arockia Jeyaprakash, A.; Jayashree, G.; Mahanta, S. K.; Swaminathan, C. P.; Sekar, K.; Surolia, A.; Vijayan, M. Structural basis for the energetics of jacalin-sugar interactions: promiscuity versus specificity. *J. Mol. Biol.* **2005**, *347*, 181−188.

(14) Komath, S. S.; Bhanu, K.; Maiya, B. G.; Swamy, M. J. Binding of porphyrins by the tumor-specific lectin, jacalin [Jack fruit (Artocarpus integrifolia) agglutinin]. *Biosci. Rep.* **2000**, *20*, 265−276.

(15) Ayaz Ahmed, K. B.; Reshma, E.; Mariappan, M.; Anbazhagan, V. Spectroscopic investigation on the interaction of ruthenium complexes with tumor specific lectin, jacalin. *Spectrochim. Acta, Part A* **2015**, *137*, 1292−1297.

(16) Ayaz Ahmed, K. B.; Mohammed, A. S.; Veerappan, A. Interaction of sugar stabilized silver nanoparticles with the T-antigen specific lectin, jacalin from Artocarpus integrifolia. *Spectrochim. Acta, Part A* **2015**, *145*, 110−116.

(17) Ahmed, K.B.A.; Subramaniyan, S. B.; Banu, S. F.; Nithyanand, P.; Veerappan, A. Jacalin-copper sulfide nanoparticles complex enhance the antibacterial activity against drug resistant bacteria via cell surface glycan recognition [published correction appears in. *Colloids Surf., B* **2018**, *163*, 209−217.

(18) Sharma, D.; Misba, L.; Khan, A. U. Antibiotics versus biofilm: an emerging battleground in microbial communities. *Antimicrob. Resist. Infect. Control* **2019**, *8*, No. 76.

(19) Gedefie, A.; Demsis, W.; Ashagrie, M.; Kassa, Y.; Tesfaye, M.; Tilahun, M.; Bisetegn, H.; Sahle, Z. *Acinetobacter baumannii* Biofilm Formation and Its Role in Disease Pathogenesis: A Review. *Infect. Drug Resist.* **2021**, *14*, 3711−3719.

(20) Strahl, H.; Errington, J. Bacterial Membranes: Structure, Domains, and Function. *Annu. Rev. Microbiol.* **2017**, *71*, 519−538.

(21) Bourne, Y.; Astoul, C. H.; Zamboni, V.; Peumans, W. J.; Menu-Bouaouiche, L.; Van Damme, E. J.; Barre, A.; Rougé, P. Structural basis for the unusual carbohydrate-binding specificity of jacalin towards galactose and mannose. *Biochem. J.* **2002**, *364*, 173−180.

(22) Karnan Singaravelu, D.; Subramaniyan, S. B.; Tharunya, M. P.; Veerappan, A. Antimicrobial lipid capped copper sulfide nanoparticles display enhanced bactericidal effect against Carbapenem-Resistant *Acinetobacter baumannii*. *Mater. Lett.* **2022**, *306*, No. 130985.
(23) Petitpas, I.; Petersen, C. E.; Ha, C. E.; Bhattacharya, A. A.; Zunszain, P. A.; Ghuman, J.; Bhagavan, N. V.; Curry, S. Structural basis of albumin-thyroxine interactions and familial dysalbuminemic hyperthyroxinemia. *Proc. Natl. Acad. Sci. U.S.A.* **2003**, *100*, 6440−6445.
(24) Pazos, I. M.; Roesch, R. M.; Gai, F. Quenching of *p*-Cyanophenylalanine Fluorescence by Various Anions. *Chem. Phys. Lett.* **2013**, *563*, 93−96.
(25) Genovese, D.; Cingolani, M.; Rampazzo, E.; Prodi, L.; Zaccheroni, N. Static quenching upon adduct formation: a treatment without shortcuts and approximations. *Chem. Soc. Rev.* **2021**, *50*, 8414−8427.
(26) Tsuji, B. T.; Yang, J. C.; Forrest, A.; Kelchlin, P. A.; Smith, P. F. In vitro pharmacodynamics of novel rifamycin ABI-0043 against *Staphylococcus aureus*. *J. Antimicrob. Chemother.* **2008**, *62*, 156−160.
(27) Klobucar, K.; Brown, E. D. New potentiators of ineffective antibiotics: Targeting the Gram-negative outer membrane to overcome intrinsic resistance. *Curr. Opin. Chem. Biol.* **2022**, *66*, No. 102099.
(28) Delcour, A. H. Outer membrane permeability and antibiotic resistance. *Biochim. Biophys. Acta, Proteins Proteomics* **2009**, *1794*, 808−816.
(29) Mizerska-Dudka, M.; Andrejko, M. Galleria mellonella hemocytes destruction after infection with *Pseudomonas aeruginosa*. *J. Basic Microbiol.* **2014**, *54*, 232−246.
(30) Subramaniyan, S. B.; Vijayakumar, S.; Megarajan, S.; Kamlekar, R. K.; Anbazhagan, V. Remarkable Effect of Jacalin in Diminishing the Protein Corona Interference in the Antibacterial Activity of Pectin-Capped Copper Sulfide Nanoparticles. *ACS Omega* **2019**, *4*, 14049−14056.
(31) Kamischke, C.; Fan, J.; Bergeron, J.; Kulasekara, H. D.; Dalebroux, Z. D.; Burrell, A.; Kollman, J. M.; Miller, S. I. The *Acinetobacter baumannii* Mla system and glycerophospholipid transport to the outer membrane. *eLife* **2019**, *8*, No. e40171.
(32) Treuner-Lange, A.; Søgaard-Andersen, L. Regulation of cell polarity in bacteria. *J. Cell Biol.* **2014**, *206*, 7−17.
(33) Jeyanthi, V.; Velusamy, P.; Kumar, G. V.; Kiruba, K. Effect of naturally isolated hydroquinone in disturbing the cell membrane integrity of *Pseudomonas aeruginosa* MTCC 741 and *Staphylococcus aureus* MTCC 740. *Heliyon* **2021**, *7*, No. e07021.
(34) Te Winkel, J. D.; Gray, D. A.; Seistrup, K. H.; Hamoen, L. W.; Strahl, H. Analysis of Antimicrobial-Triggered Membrane Depolarization Using Voltage Sensitive Dyes. *Front. Cell. Dev. Biol.* **2016**, *4*, No. 29.
(35) Zhao, X.; Drlica, K. Reactive oxygen species and the bacterial response to lethal stress. *Curr. Opin. Microbiol.* **2014**, *21*, 1−6.
(36) Seo, Y.; Park, K.; Hong, Y.; Lee, E. S.; Kim, S. S.; Jung, Y. T.; Park, H.; Kwon, C.; Cho, Y. S.; Huh, Y. D. Reactive-oxygen-species-mediated mechanism for photoinduced antibacterial and antiviral activities of Ag_3PO_4. *J. Anal. Sci. Technol.* **2020**, *11*, No. 21.
(37) Ong, K. S.; Cheow, Y. L.; Lee, S. M. The role of reactive oxygen species in the antimicrobial activity of pyochelin. *J. Adv. Res.* **2017**, *8*, 393−398.
(38) Qi, L.; Li, H.; Zhang, C.; Liang, B.; Li, J.; Wang, L.; Du, X.; Liu, X.; Qiu, S.; Song, H. Relationship between Antibiotic Resistance, Biofilm Formation, and Biofilm-Specific Resistance in *Acinetobacter baumannii*. *Front. Microbiol.* **2016**, *7*, No. 483.
(39) Selvaraj, A.; Valliammai, A.; Sivasankar, C.; Suba, M.; Sakthivel, G.; Pandian, S. K. Antibiofilm and antivirulence efficacy of myrtenol enhances the antibiotic susceptibility of *Acinetobacter baumannii*. *Sci. Rep.* **2020**, *10*, No. 21975.
(40) Costa, P.; Gomes, A.; Braz, M.; Pereira, C.; Almeida, A. Application of the Resazurin Cell Viability Assay to Monitor *Escherichia coli* and *Salmonella* Typhimurium Inactivation Mediated by Phages. *Antibiotics* **2021**, *10*, 974.
(41) Raorane, C. J.; Lee, J. H.; Kim, Y. G.; Rajasekharan, S. K.; García-Contreras, R.; Lee, J. Antibiofilm and Antivirulence Efficacies of Flavonoids and Curcumin Against *Acinetobacter baumannii*. *Front. Microbiol.* **2019**, *10*, No. 990.
(42) Limoli, D. H.; Jones, C. J.; Wozniak, D. J. Bacterial Extracellular Polysaccharides in Biofilm Formation and Function *Microbiol. Spectrum* 2015, *3*, 3, 10.1128 DOI: 10.1128/microbiolspec.MB-0011-2014.
(43) May, H. C.; Yu, J. J.; Shrihari, S.; Seshu, J.; Klose, K. E.; Cap, A. P.; Chambers, J. P.; Guentzel, M. N.; Arulanandam, B. P. Thioredoxin Modulates Cell Surface Hydrophobicity in *Acinetobacter baumannii*. *Front. Microbiol.* **2019**, *10*, No. 2849.
(44) Corral, J.; Pérez-Varela, M.; Sánchez-Osuna, M.; Cortés, P.; Barbé, J.; Aranda, J. Importance of twitching and surface-associated motility in the virulence of *Acinetobacter baumannii*. *Virulence* **2021**, *12*, 2201−2213.
(45) Torraca, V.; Mostowy, S. Zebrafish Infection: From Pathogenesis to Cell Biology. *Trends Cell Biol.* **2018**, *28*, 143−156.
(46) Neely, M. N.The Zebrafish as a Model for Human Bacterial Infections. In *Bacterial Pathogenesis*; Methods in Molecular Biology; Springer, 2017; Vol. *1535*, pp 245−266.

https://doi.org/10.1021/acsomega.2c05252
ACS Omega 2022, 7, 43934−43944